Exp Brain Res (2009) 199:345–353
DOI 10.1007/s00221-009-1722-8

RESEARCH ARTICLE

Shift of chloride reversal potential in neurons of the accessory optic system in albinotic rats

Martin Krause · Klaus-Peter Hoffmann

Received: 28 October 2008 / Accepted: 18 January 2009 / Published online: 12 February 2009

Abstract Albinism affects the anatomy and physiology of the visual system in mammals. Behavioural, anatomical and in vivo electrophysiological investigations revealed that the optokinetic reflex is abnormal and retinal slip neurons in the nucleus of the optic tract and the dorsal terminal nucleus of the accessory optic system (NOT-DTN) lack direction selectivity and have a reduced dendritic tree in albinotic rats and ferrets. Earlier investigations show a disturbed chloride homeostasis and a depolarizing action of GABAergic currents in visual cortex cells of albinotic rats. We assume that an altered local inhibition could be one critical factor explaining the loss of direction selecitivity in DTN neurons. To test this patch clamp analysis of NOT-DTN neurons in 250 μm thick acute brain slices from pigmented and albinotic rats were performed. GABAergic IPSCs were elicited by lateral current stimulation and the reversal potentials of $GABA_A$-mediated currents (E_{GABA}) were determined. Our results show a significantly more negative E_{GABA} in NOT-DTN neurons of pigmented (−62.1 mV, ±10.8 mV, $n = 24$) than of albinotic rats (−49.2 mV, ±17.7 mV, $n = 19$; $P < 0.001$). Control measurements in the superficial layer of the superior colliculus revealed no significant differences between pigmented (−56.2 mV, ±16.4 mV, $n = 17$) and albinotic rats (−60.7 mV, ±13.8 mV, $n = 28$; $P > 0.324$). A similar shift in reversal potential of $GABA_A$-mediated currents was observed also in pyramidal cells in layers II/III and V of the visual cortex and was explained by an accumulation of intracellular chloride due to an abnormal activity of chloride co-transporters. As described for retinal ganglion cells and cortical neurons, direction selectivity is formed by a balanced excitatory and inhibitory input. Our combined data suggest that the observed shift in reversal potential and a possible dysfunction of inhibitory interneurons might indeed be one factor responsible for the reduction of direction selectivity in the NOT-DTN and therefore for the pathology of the optokinetic response in albino mammals.

Keywords Albinism · Optokinetic response · Accessory optic system · Colliculus superior · GABA

Abbreviations

aCSF	Artificial cerebrospinal fluid
AOS	Accessory optic system
$[Cl^-]_i$	Intracellular chloride concentration
DSGC	Direction-selective ganglion cell
E_{GABA}	Reversal potential of GABA mediated currents
GABA	Gamma-aminobutryc acid
KCC2	K^+–Cl^- co-transporter type 2
LTN	Lateral terminal nucleus of AOS
MTN	Medial terminal nucleus of AOS
NKCC1	Na^+–K^+–$2Cl^-$ co-transporter type 1
NOT-DTN	Nucleus of the optic tract and dorsal terminal nucleus
OKN	Optokinetic nystagmus

Introduction

The accessory optic system (AOS) of mammals consists of four distinct nuclei: the dorsal terminal nucleus (DTN), the medial terminal nucleus (MTN), the lateral terminal nucleus (LTN) and the interstitial nucleus of the superior fasciculus, posterior fibres (inSFpf). These nuclei receive direct retinal projections from direction-selective ganglion

M. Krause (✉) · K.-P. Hoffmann
Department of General Zoology and Neurobiology,
Ruhr-University Bochum, ND 7/31, 44780 Bochum, Germany
e-mail: martin.krause@rub.de; krause@neurobiologie.rub.de

cells (for reviews see Simpson 1984; Giolli et al. 2005). Neurons in the AOS are direction-selective and respond to slip of the image of the world on the retina. Retinal slip neurons in the nucleus of the optic tract and the associated DTN (NOT-DTN) strongly respond to ipsiversive horizontal pattern motion, with neurons in the left NOT-DTN preferring movement to the left, and vice versa. The NOT-DTN neurons project to the inferior olive, the dorsolateral pontine nucleus, the nucleus reticularis tegmenti pontis, and the nucleus praepositus hypoglossi (Magnin et al. 1989). In addition, neurons in the structure equivalent to the mammalian NOT in non-mammals terminate also directly on extraocular motoneurons; e.g., the nucleus abducens in frog and fish. Visual motion information is then transferred via the vestibular nuclei to the oculomotor nuclei innervating the extraocular muscles. In the neuronal circuit underlying the horizontal optokinetic nystagmus (OKN) the NOT-DTN represents the visuomotor interface (e.g., Simpson 1984). Albinotic mammals show, amongst other disorders of the visual system, strongly reduced ability to perceive visual motion and to stabilize their visual environment on the retina (Lannou et al. 1982; Hoffmann et al. 2004; Hupfeld and Hoffmann 2006; Hupfeld et al. 2007). In vivo electrophysiological measurements in albinotic rats and ferrets revealed that retinal slip neurons in the NOT-DTN lack direction selectivity (Lannou et al. 1982; Hoffmann et al. 2004). To date, it is not clear if these abnormalities are caused in the NOT-DTN itself or whether they are the consequence of altered retinal or cortical inputs. Anatomical studies showed a shrunken dendritic network in the NOT-DTN of albinotic ferrets (Telkes et al. 2001). It is unclear whether these findings reflect altered inputs and how they could be related to the lack of direction selectivity.

To shed more light on the electrophysiological properties of NOT-DTN cells in albinotic animals, we performed patch clamp experiments in slice preparations and compared the biophysical and synaptic characteristics of DTN cells of pigmented Longs Evans and albinotic Wistar rats. Direction selectivity is strongly related to GABAergic mechanisms and the activity of chloride co-transporters (Caldwell et al. 1978; Schmidt et al. 1994; Kittila and Massey 1997; Taylor et al. 2000; Gavrikov et al. 2003; Thiele et al. 2004). Inhibitory interneurons play an important role in the computation of direction-selective responses of retinal ganglion cells and visual cortex neurons (for example Fried et al. 2002; Priebe and Ferster 2005). A separation of preferred and non-preferred directions is formed by the balance of excitatory and inhibitory inputs. We postulate that a dysfunction of the inhibitory mechanism directly impacts direction selectivity in DTN neurons.

Former studies on pyramidal cells in visual cortical layers II/III and V showed a shift of the reversal potential of $GABA_A$-mediated currents in albinotic rats (Barmashenko et al. 2005). Pharmacological characterisation of this shift with blockers of chloride co-transporters indicated an increased activation of inward-directed chloride transporter NKCC1 and a reduced activation of the outward-directed transporter KCC2, leading to an increased intracellular chloride concentration. Our working hypothesis is that the inhibitory action of GABA is diminished by this increased intracellular chloride concentration. However, no link has been found between the genetic mutation leading to albinism and the regulation of chloride homeostasis on the cellular level. First evidence for alterations of excitatory and inhibitory mechanisms comes from the finding that the ratio of glutamate to GABA is altered in the retina of albinotic rats compared with pigmented ones (Blaszczyk et al. 2004). To investigate if the lack of direction selectivity in albinos can be explained by a disinhibition of NOT-DTN cells, we measured the reversal potential of $GABA_A$-mediated currents and the direction of the shift in membrane potential after GABA release from presynaptic cells.

Materials and methods

In vitro electrophysiological experiments were performed on acute brain slices from P21–P35 pigmented Long-Evans rats (HsdBlu:LE) and albino Wistar Unilever rats (HsdCpb:WU) of either sex. Animals were purchased from Harlan–Winkelmann (Borchen, Germany) or bred and raised in the institute's animal facility. All experimental procedures were approved by the local authorities (Regierungspräsidium Arnsberg) and were performed in accordance with the European Communities Council directive of 24 November 1986 (S6609 EEC) and National Institutes of Health guidelines for care and use of animals for experimental procedures.

Slice preparation

Animals were deeply anaesthetised with halothane, and a subcutaneous injection of ketamine hydrochloride (100 mg/kg body weight) and thiazine hydrochloride (1 mg/kg body weight) and perfused transcardially with carbogene (5% CO_2, 95% O_2) saturated, ice-cold artificial cerebrospinal fluid [aCSF (in mM): NaCl, 123; KCl, 2.5; NaH_2PO4, 1; $NaHCO_3$, 26; D-glucose, 11; $CaCl_2$, 1.8; $MgCl_2$, 1.3; pH 7.4]. After perfusion, the brain was quickly removed, immersed in ice-cold aCSF and prepared for slicing. On a vibratome (MA752, Campden Instruments, UK) 250 µm thick coronal slices containing the superior colliculus (SC) and the DTN were cut from Bregma −7.5 to −6.0 mm (Paxinos et al. 1985). After incubation at room temperature for at least 1 h slices were transferred to a recording chamber integrated on the fixed stage of an upright microscope (Olympus BX-51 WI, Olympus, Japan). The recording

chamber was continuously perfused with aCSF at 3 ml/min. All recordings were performed at room temperature.

Recordings

Perforated patch clamp recordings were performed using borosilicate glass pipettes pulled on a vertical puller (PIP5, HEKA, Germany) and filled with a pipette solution containing (in mM): K-gluconate, 130; Na-gluconate, 0.5; HEPES, 20; $MgCl_2$, 4; Na_2ATP, 4; Na_3GTP, 0.4; EGTA, 0.5 (pH 7.2). To avoid changes of intracellular chloride concentration gramicidin A was added to achieve membrane perforation. A stock solution of gramicidin A (10 mg/ml in DMSO) was diluted in 1 ml pipette solution to obtain a final concentration of 52 µg/ml and treated with ultrasound for 5 min. This procedure was repeated every 2 h due to observed precipitation of gramicidin in the pipette solution. The sodium channel blocker QX-314 was added to the pipette solution (5 mM) for verification of the patch integrity.

Cells were measured in voltage clamp mode using a patch clamp amplifier (PC-501A, Warner Instruments, USA) connected to a personal computer via AD/DA-converter (CED 1401+, Cambridge Electronic Design, UK). After performing a giga-seal configuration, integration of gramicidin into the membrane was observed by a drop in access resistance using hyperpolarizing voltage steps of −5 mV. A stable perforated patch was obtained after 20–30 min incorporation time. Physiological membrane characteristics were measured using de- and hyperpolarizing voltage steps of different time lengths. The threshold for action potential dependent sodium currents was determined by the application of voltage ramps. Postsynaptic currents were elicited by lateral current stimulation (100 µA, 300 µs duration, 0.1 Hz) via a bipolar tungsten electrode 200 µm apart from the recorded cell. All glutamatergic postsynaptic currents were blocked by the application of 2 mM kynurenic acid (Sigma). The amplitude of $GABA_A$-mediated postsynaptic currents was measured at different holding potentials in the range from −100 to +20 mV with step intervals of 10 mV. The reversal potential of these currents was calculated by linear regression analysis of the current-voltage relationship. After measurements, the perforated patch was ruptured by the application of negative pressure to the recording pipette. In whole-cell configuration measurements were repeated immediately and after a waiting period of 10 min. All measured potentials were corrected for the junction potential of −10 mV.

Morphological reconstruction

In most of the experiments biocytin (Sigma, 10 mg/ml) was added to the pipette solution and diffused into cells during measurements in whole-cell configuration. At the end of the experiment, slices were fixed in 4% paraformaldehyde and recorded cells were stained using 3,3-diaminobenzidine to verify their location inside of the DTN or the superficial grey of the superior colliculus (Fig. 1).

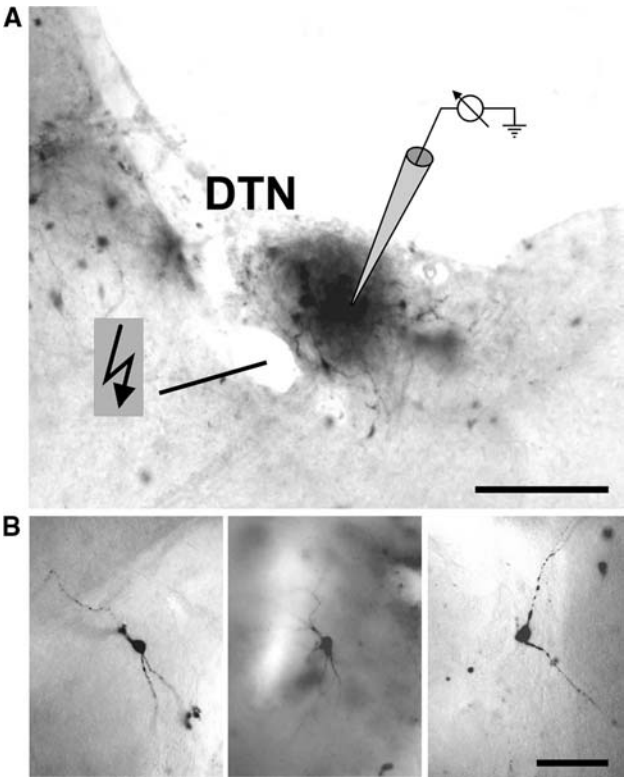

Fig. 1 **a** Semischematic illustration of electrophysiological measurements in the dorsal terminal nucleus (*DTN*). The dorsal terminal nucleus as a part of the accessory optic system is localised between the superior colliculus and the medial geniculate body (not shown). Gramicidin perforated patch clamp measurements were performed within the DTN with electrical stimulation lateral to the measured cell to evoke GABAergic currents. Cells were stained with DAB after pressure injection of biocytin into the slice for localisation of the DTN. **b** DTN cells from albinotic rats, intracellularly filled with biocytine after recordings. *Scale bars* represent 200 µm (**a**) and 50 µm (**b**)

Results

Electrophysiological measurements of passive membrane properties and the reversal potential of $GABA_A$-related currents were performed in cells in the DTN and the superficial grey of the colliculus superior in albinotic and pigmented rats. In the DTN, 39 cells from pigmented and 30 cells from albinotic animals were characterised. In the SC, 26 cells from pigmented and 45 cells from albinotic animals were investigated. No quantitative analysis of different cell types within the SC was performed due to the relatively low cell numbers. Biocytin staining was performed and cells recorded outside the DTN or the SC were excluded from further analysis. In addition, neurons with a resting potential

Table 1 Electrophysiological characterisation of cells in the dorsal terminal nucleus (DTN) and the superficial layers of the superior colliculus (SC) from pigmented and albino rats

	Pigmented	SD	*n*	Albino	SD	*n*
DTN						
Resting potential	−61.7 mV	±3.93 mV	39	−58.1 mV	±12.4 mV	30
Input resistance	360.5 MΩ	±146.6 MΩ	28	438.2 MΩ	±195.7 MΩ	24
Spike threshold	−25.8 mV	±10,2 mV	12	−26.24 mV	±8.16 mV	10
E_{GABA}	−62.1 mV	±10.8 mV	24	−49.2 mV	±17.7 mV	19
SC						
Resting potential	−59.4 mV	±11.3 mV	26	−60.7 mV	±10.8 mV	45
Input resistance	412.5 MΩ	±206.9 MΩ	16	550 MΩ	±144.5 MΩ	21
Spike threshold	−40.3 mV	±10.4 mV	11	−39.5 mV	±9.4 mV	16
E_{GABA}	−56.2 mV	±16.4 mV	17	−60.7 mV	±13.8 mV	28

Only the difference in E_{GABA} measured in DTN cells is statistically significant ($P < 0.001$)

Data represent mean values with standard deviations (*SD*) and number of measured cells (*n*)

of less than −40 mV or a sudden drop of input resistance during the measurements due to a rupture of the gramicidin perforated patch were excluded.

In the first set of experiments, we compared the passive membrane properties of recorded cells during patch clamp measurements in voltage clamp whole-cell configuration. No significant difference in input resistance or spike threshold was found for DTN cells or SC cells from pigmented and albinotic animals. In DTN cells of albinos a non-significant trend to more positive values of resting potential compared to pigmented rats was observed. Spike thresholds of DTN cells were more positive than those of SC neurons (for values see Table 1).

In a second set of experiments, we measured the amplitude of $GABA_A$-related IPSCs at different holding potentials and calculated the reversal potential of these currents (E_{GABA}). Glutamatergic currents were blocked by the application of kynurenic acid. Figure 2 shows representative DTN cells from albino and pigmented rats. After application of 20 µM bicuculline evoked currents disappeared, confirming that measured IPSCs were $GABA_A$ related (Fig. 2b, inset). Same result was obtained by the application of 100 µM picrotoxin (not shown).

For collicular neurons, no statistically significant differences of E_{GABA} were found between pigmented and albino animals (Fig. 3a; Table 1) (pigmented −56.2 ± 16.4 mV, $n = 17$; albino −60.7 ± 13.8 mV, $n = 28$). Individual values of E_{GABA} varied largely in both phenotypes as indicated by the standard deviations. We did not attempt to correlate E_{GABA} with different collicular cell types according to Langer and Lund (1974) because of our low cell numbers.

In contrast, E_{GABA} of DTN cells of pigmented rats was significantly more negative in pigmented (−62.1 mV, ±10.8 mV, $n = 24$) than in albinotic rats (−49.2 mV,

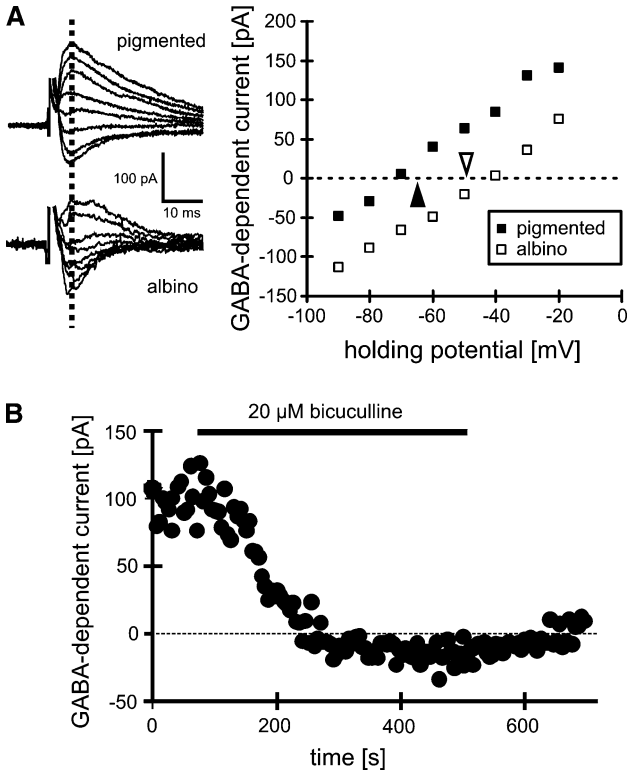

Fig. 2 **a** Sample traces of the electrically evoked $GABA_A$ receptor-mediated postsynaptic currents in DTN neurons from pigmented and albino rats and corresponding current-voltage relationships from the same cells. In perforated patch, cells were clamped at different holding potentials and GABA mediated currents were elicited by current stimulation. The reversal potential of $GABA_A$ dependent current was more positive in the cell from the albino rat. *Arrows* indicate mean reversal potentials from all measured cells. **b** Application of the $GABA_A$ antagonist bicuculline (20 µM) blocks postsynaptic currents, indicating that measured currents are GABA-dependent. The *black* represents the application time. Postsynaptic currents were measured continuously at intervals of 5 s and a holding potential of −30 mV

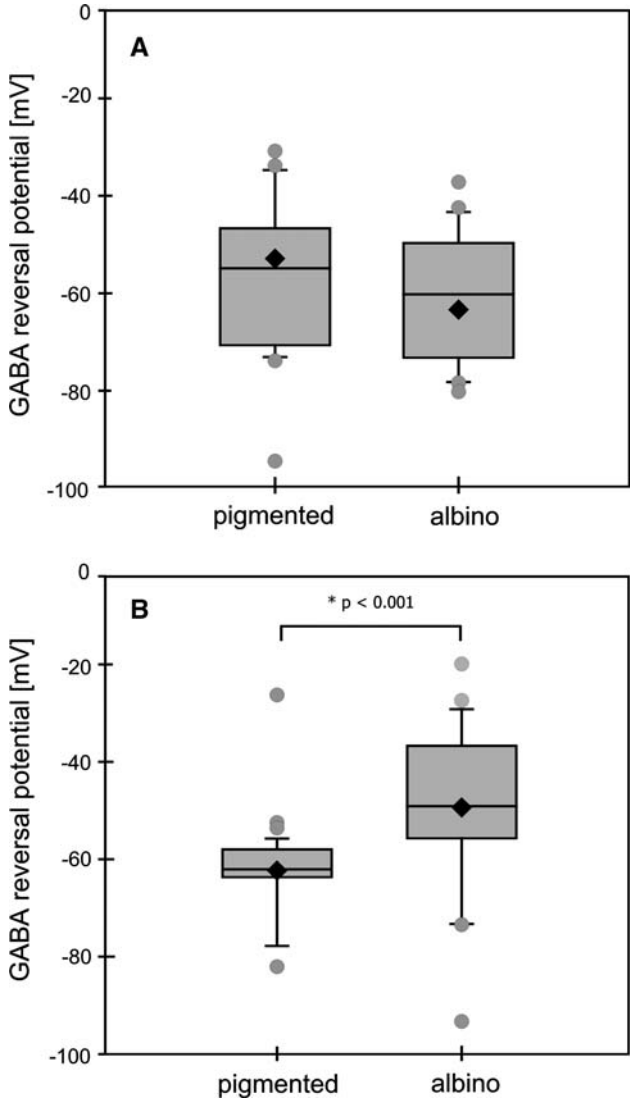

Fig. 3 Reversal potential of $GABA_A$-related currents (E_{GABA}). *Box* plots show median values and confidence ranges. *Black diamonds* represent the mean value. For exact values see also Table 1. **a** No significant difference was found in cells from superficial layers of superior colliculus from albino (28 cells) and pigmented rats (17 cells). **b** DTN cells from albino (19 cells) and pigmented rats (24 cells) show a significant ($P < 0.001$) difference in their E_{GABA}. In albino rats, a higher variation of reversal potentials between individual cells was found

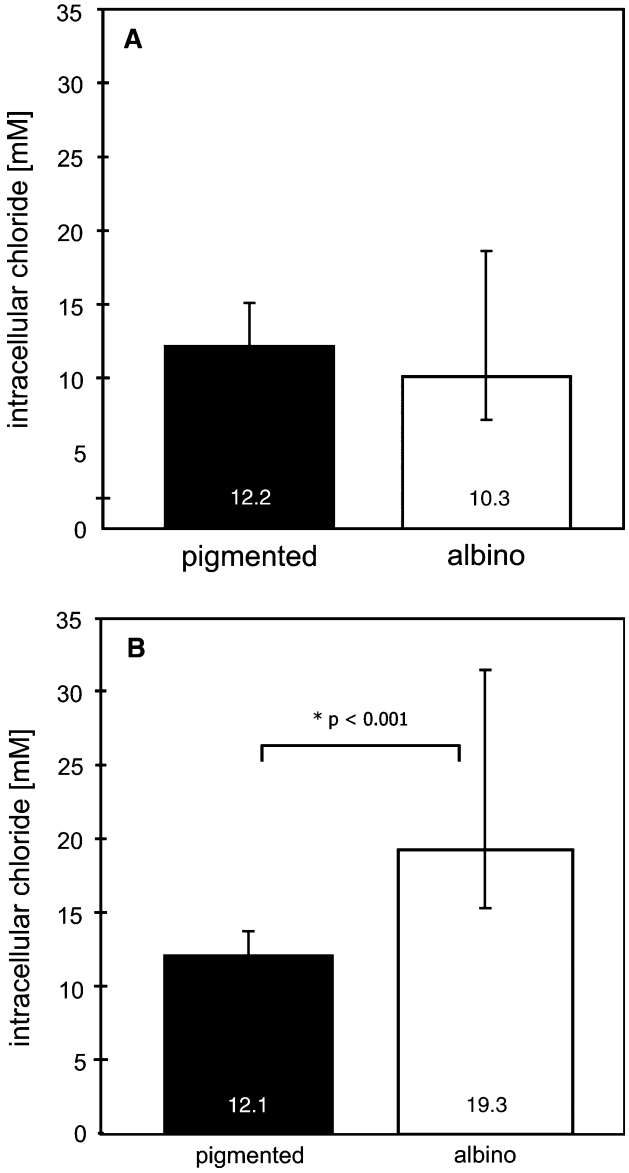

Fig. 4 Median intracellular chloride concentration in superior colliculus cells (**a**) and DTN cells (**b**) from albino and pigmented rats. In DTN cells from albino rats $[Cl^-]_i$ is significantly increased. In pigmented rats $[Cl^-]_i$ was found to be in the same range as in cells from superficial layers of the superior colliculus. The increase in intracellular chloride in albino DTN cells leads to the significant shift of reversal potential of $GABA_A$-related currents (*cell numbers* as in Fig. 3)

±17.7 mV, $n = 19$; $P < 0.001$). Thus, the reversal potential of GABA-related currents in albinotic rats is shifted to more positive values and individual values of E_{GABA} are more variable than in pigmented rats (Fig. 3b; Table 1).

In addition, we calculated the mean intracellular chloride concentration for DTN and SC cells using the Nernst equation (Fig. 4). In the superior colliculus no significant difference was found between pigmented (12.2 mM) and albino rats (10.3 mM) (Fig. 4a). The intracellular chloride concentration of DTN cells of pigmented rats was 12.1 mM corresponding to the concentration in SC cells. In DTN cells of albino rats, however, $[Cl^-]_i$ was significantly elevated to a mean concentration of 19.3 mM ($P < 0.001$).

As a control for our recording technique, we switched to whole-cell configuration by applying negative pressure to the patch pipette after completion of the measurements in the perforated patch configuration. We determined E_{GABA} of DTN cells immediately (Fig. 5a) and 10 min after rupturing the cell membrane (Fig. 5b). With this procedure, intracellular chloride equilibrates with the chloride concentration in the patch pipette. Immediately after the switch,

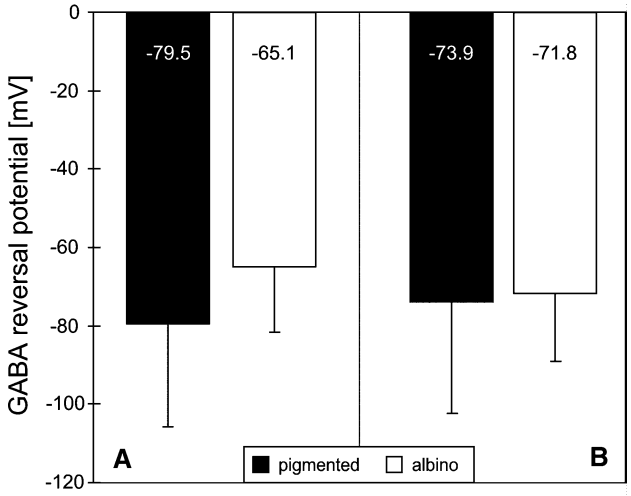

Fig. 5 Reversal potentials of $GABA_A$ dependent currents in DTN cells measured in whole-cell configuration immediately (**a**) and 10 min after rupturing the perforated patch (**b**). In whole-cell configuration intracellular chloride adapts to the chloride concentration in the patch pipette. In (**b**) no difference was found in E_{GABA} between cells from pigmented and albino rats. The values for E_{GABA} (−73.9 mV in pigmented, −71.8 mV in albino) correspond to $[Cl^-]_i$ of 7.6 and 7.9 mM which is close to the $[Cl^-]$ in the pipette solution (8 mM)

the reversal potential of $GABA_A$-related currents was shifted to more negative values in cells of pigmented (−79.5 mV) and of albino rats (−65.1 mV). The difference between the phenotypes was not statistically significant any more and vanished completely after 10 min in whole-cell configuration (pigmented: −73.9 mV, albino: −71.8 mV). These experiments revealed two facts: first, the measured reversal potentials after 10 min whole-cell configuration corresponded to an intracellular chloride concentration close to the concentration in the pipette solution (8 mM) indicating that the influence of additional ion conductance like bicarbonate was relatively small. Second, the reversal potentials of cells from both pigmented and albino rats measured in whole-cell configuration as shown in Fig. 5b differ from the values measured with gramicidin indicating the integrity of the perforated patch configuration. A possible leakage during gramicidin measurements should lead to a chloride diffusion and shift the E_{GABA} measured under perforated patch conditions to values obtained under whole-cell configuration.

To determine the relationship of GABA activation and the resting potential of collicular and DTN cells we plotted E_{GABA} versus the resting potential of each individual cell (Fig. 6). If E_{GABA} is more negative than the cell's resting potential, GABA leads to a hyperpolarisation. Is E_{GABA} more positive than the neuron's resting potential GABA leads to a depolarisation of the cell. The dotted line in Fig. 6 indicates the unity slope where GABA activation leads to no change in resting potential. For the superior colliculus data points were equally distributed around the unity slope (Fig. 6b). In ten cells from pigmented rats GABA led to depolarisation, whereas in six cells GABA led to hyperpolarisation of the membrane potential. In albino rats, 13 cells depolarised and 14 cells hyperpolarised after GABA activation. There was no statistically significant difference between pigmented and albino rats (exact Fisher test, $P < 0.23$). In contrast, data points of DTN cells show a different distribution around the unity slope (Fig. 6a). In 14 out of 17 cells of albinotic rats GABA led to depolarisation of the membrane potential, whereas values obtained from pigmented rats were equally distributed. Ten cells showed a depolarisation, and ten cells showed a hyperpolarisation after GABA activation. Application of the exact Fisher test reveals a statistically different distribution ($P < 0.04$) between cells from pigmented and albino rats. Statistical analysis of the distribution between SC and DTN revealed no difference in pigmented rats ($P < 0.34$) but a significant difference in albinotic rats ($P < 0.02$).

Discussion

In all mammals investigated so far albinism has a profound effect on the morphology and the functional properties of the visual system. For the Wistar rat used in this study the mutation leading to oculocutaneous albinism was identified recently (Blaszczyk et al. 2005). It is commonly accepted that spatiotemporal alteration of neurogenesis caused by a reduction in L-DOPA (dihydroyphenylalanine) leads to a reduction of rods and ganglion cells in the albino retina and to an abnormal crossing of retinofugal fibres from the temporal retina (e.g., Jeffery 1997; Rachel et al. 2002). In albino ferrets ipsilateral retinal projections to the superior colliculus, the pretectal area and to the visual thalamus show a remarkable reduction (Morgan et al. 1987; Zhang and Hoffmann 1993). Recent experiments using retrograde tracing techniques revealed that in albino ferrets a population of retinal ganglion cells projects simultaneously to the NOT-DTN and to the MTN indicating a reduced specificity of these cells (Distler et al., this issue).

In contrast, much less is known about the effect of albinism on the physiology of individual cells. In this study, we found that the reversal potential of $GABA_A$-related currents of DTN cells of albinotic rats is significantly shifted to more positive values. This result is in-line with the earlier investigations by Barmashenko et al. (2005) who found similar results for pyramidal cells in layers II/III and V of the visual cortex. This difference was tentatively explained by an altered balance between inwardly and outwardly acting chloride co-transporters (Diykov et al. 2008a). The changes in E_{GABA} after pharmacological blocking of the co-transporters NKCC1 and KCC2 led to the assumption that

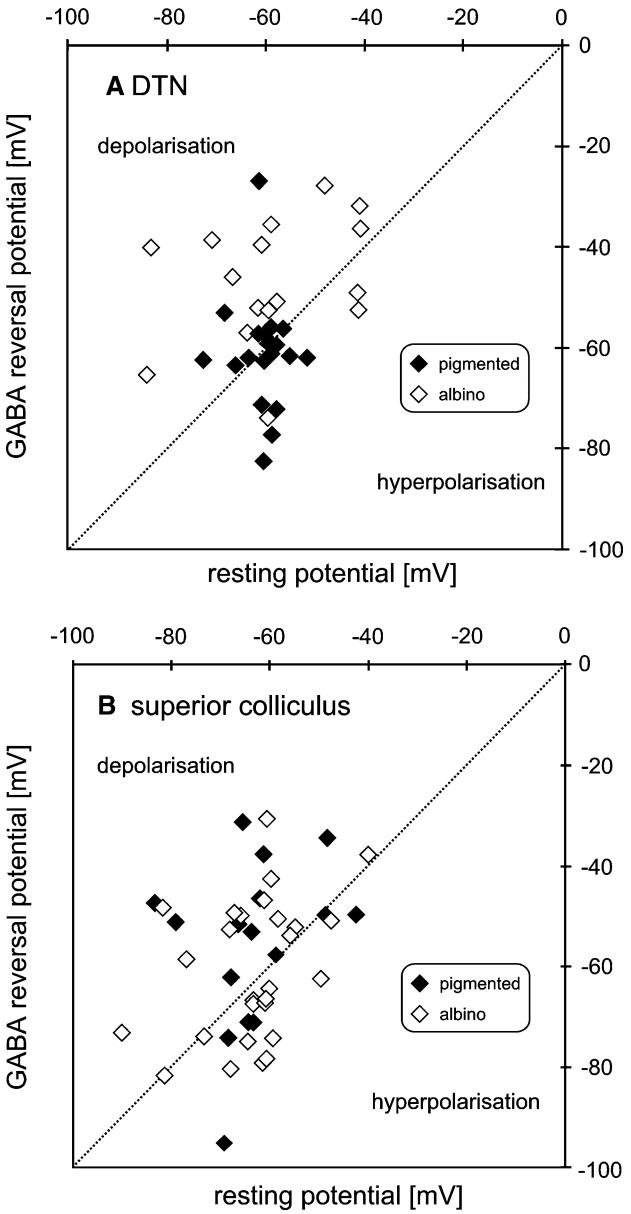

Fig. 6 *Scatter plots* of E_{GABA} and resting potentials for DTN (**a**) and superior colliculus (**b**) neurons. *Dotted line marks* represent the unity slope, where GABA activation leads to no change in membrane potential. *DTN* neurons from pigmented rats show resting potentials more positive than E_{GABA}, and $GABA_A$ activation leads to a hyperpolarisation. In contrast, most cells from albino rats have a significant shift of E_{GABA} to more positive values, and $GABA_A$ activation leads to a depolarisation. When compared with cells from pigmented rats resting potentials and E_{GABA} in cells from albino rats show a higher variation. In the superficial layer of the superior colliculus no significant differences between the two populations of cells occurred

the chloride homeostasis of neurons in the visual cortex of albino rats corresponds to that of immature neurons. A further developmental study confirms these results (Diykov et al. 2008b). An increased activity of NKCC1 and/or a reduction in the activity of KCC2 leads to a high intracellular chloride concentration (Kaila 1994; Kakazu et al. 1999; Ben-Ari 2002; Yamada et al. 2004) shifting the reversal potential for $GABA_A$-related currents to more positive values. Because in visual cortical neurons no difference in excitatory postsynaptic currents was found between albino and pigmented rats (Barmashenko et al. 2005), we did not perform such measurements in DTN cells.

The differences in E_{GABA} between DTN cells of pigmented and albino rats raise the question about the physiological consequences of this alteration in chloride homeostasis. The resting potentials of DTN cells were not different between pigmented and albino rats. This result is in contrast to the results of Barmashenko et al. (2005) who found also significant differences in resting potential and rheobase (current threshold for spike release after long depolarizing pulses). However, an alteration of intracellular chloride concentration can invert the electromotoric force for $GABA_A$-related currents if the shift of the reversal potential is strong enough and the resting potential is more or less constant. A reversal potential of $GABA_A$-mediated currents more negative than the resting potential leads to hyperpolarisation and possibly to a decreased probability of action potential generation in postsynaptic cells. A shift of the reversal potential to values more positive than the resting potential leads to depolarisation, which could result in an increased probability of action potential generation in postsynaptic cells. During our experiments no increased spiking behaviour was found in cells from albino animals. The reversal potential of GABA-dependent currents is more negative than the threshold for spike generation (Table 1) indicating that the electromotive force is not strong enough to increase the overall excitability in most of the postsynaptic cells. A further important point is that the GABA activation not only depolarizes the postsynaptic cell but also decreases the input resistance and shunts excitatory as well as inhibitory inputs. If GABA is postulated to act excitatory it has to overcome shunting inhibition as described for immature neuronal systems (Cherubini et al. 1990; Ben-Ari 2002) or neurons that initiate epileptic activity (e.g., Palma et al. 2006).

Our results show that in the DTN of albinotic rats most cells show depolarisation after GABA activation. This is in contrast to DTN cells of pigmented rats and to SC cells of both phenotypes. The direction selectivity of DTN neurons is generated by an excitatory input from ON-type direction-selective retinal ganglion cells and its integration with the background activity of the DTN neurons (for a model see Simpson 1984). The directional tuning of the DTN neurons is in addition modulated by inhibitory interneurons within the AOS (Simpson et al. 1979). We propose that the shift of E_{GABA} is at least one mechanism that could lead to the diminished direction selectivity of DTN cells due to unspecific generation of action potentials even in the null direction which normally is specified by GABAergic inhibition

(Schmidt et al. 1994; Thiele et al. 2004) This would eliminate the direction-specific activity differences between the left and right DTN during unidirectional retinal slip and thereby abolish OKN in albino animals (Lannou et al. 1982, Hoffmann et al. 2004). It is generally acknowledged that direction selectivity in the retina and the visual cortex critically depends on GABAergic mechanisms (e.g., Caldwell et al. 1978; Kittila and Massey 1997; Taylor et al. 2000; Gavrikov et al. 2003; Thiele et al. 2004). Application of GABA antagonists diminishes direction selectivity of retinal ganglion cells (Schuerger et al. 1990; Kittila and Massey 1997; Smith et al. 1996). Recent investigations show that differential distribution of chloride co-transporter on the dendrites of retinal starburst amacrine cells mediates direction selectivity (Gavrikov et al. 2003). ON-type direction-selective ganglion cells (DSGCs) project to the AOS and thus to the DTN (Oyster et al. 1980; Buhl and Peichl 1986; Dann and Buhl 1987; Hoffmann and Stone 1985). DSGCs in the mouse retina were tested for their direction selectivity and showed relative broad tuning curves (Sun et al. 2006). For the generation of OKN, a sharpening of the broadly tuned retinal input in the accessory system should be of advantage. The retinal input to the NOT-DTN and the AOS is excitatory. For the formation of sharply tuned direction selectivity within the NOT-DTN the involvement of inhibitory interneurons has to be postulated. The observed changes in E_{GABA} in DTN neurons of albinotic rats could have a significant effect on the inhibitory action of these interneurons. Further experiments should answer the question if direction selectivity in the albino retina is disturbed and if the loss of direction selectivity in the DTN might be a consequence of both the change in E_{GABA} and a defective retinal input. Obviously, albinism affects different visual subsystems in a non-uniform manner as E_{GABA} of SC cells did not differ between pigmented and albino rats.

In conclusion, our results show that the lack of direction selectivity in the NOT-DTN of albino mammals can at least in part be ascribed to an altered chloride homeostasis of the cells that would then mediate non-direction selective signals to the oculomotor system. A putative additional involvement of a defective retinal input demands further investigations of DSGCs in the albino retina.

Acknowledgments We thank Margareta Möllmann and Martina Silczak for technical assistance. This work was supported by a grant from the Deutsche Forschungsgemeinschaft (SFB 509, 'Neurovision', TP A11).

References

Barmashenko G, Schmidt M, Hoffmann K-P (2005) Differences between cation-chloride co-transporter functions in the visual cortex of pigmented and albino rats. Eur J NeuroSci 21:1189–1195

Ben-Ari Y (2002) Excitatory actions of GABA during development: the nature of the nurture. Nat Rev Neurosci 3:728–739

Blaszczyk WM, Straub H, Distler C (2004) GABA content in the retina of pigmented and albino rats. NeuroReport 15:1141–1144

Blaszczyk WM, Arning L, Hoffmann K-P, Epplen JT (2005) A tyrosinase missense mutation causes albinism in the Wistar rat. Pigment Cell Res 18:144–145

Buhl EH, Peichl L (1986) Morphology of rabbit retinal ganglion cells projecting to the medial terminal nucleus of the accessory optic system. J Comp Neurol 253:163–174

Caldwell JH, Daw NW, Wyatt HJ (1978) Effects of picrotoxin and strychnine on rabbit retinal ganglion cells: lateral interactions for cells with more complex receptive fields. J Physiol 276:277–298

Cherubini E, Rovira C, Gaiarsa JL, Corradetti R, Ben Ari Y (1990) GABA mediated excitation in immature rat CA3 hippocampal neurons. Int J Dev Neurosci 8(4):481–490

Dann JF, Buhl EH (1987) Retinal ganglion cells projecting to the accessory optic system in the rat. J Comp Neurol 262:141–158

Diykov D, Turchinovich A, Zoidl G, Hoffmann K-P (2008a) Elevated intracellular chloride level in albino visual cortex neurons is mediated by Na–K–Cl co-transporter. BMC Neurosci 9:57

Diykov D, Barmashenko G, Hoffmann K-P (2008b) Development of chloride homeostasis in albino and pigmented rat visual cortex neurons. NeuroReport 19(5):595–598

Fried SI, Münch TA, Werblin FS (2002) Mechanisms and circuitry underlying directional selectivity in the retina. Nature 420(6914):411–414

Gavrikov KE, Dmitriev AV, Keyser KT, Mangel SC (2003) Cation-chloride cotransporters mediate neural computation in the retina. Proc Natl Acad Sci USA 100:16047–16052

Giolli RA, Blanks RH, Lui F (2005) The accessory optic system: basic organization with an update on connectivity, neurochemistry, and function. Prog Brain Res 151:407–440

Hoffmann K-P, Stone J (1985) Retinal input to the nucleus of the optic tract of the cat assessed by antidromic activation of ganglion cells. Exp Brain Res 59:395–403

Hoffmann K-P, Garipis N, Distler C (2004) Optokinetic deficits in albino ferrets (*Mustela putorius furo*): a behavioral and electrophysiological study. J Neurosci 24:4061–4069

Hupfeld D, Hoffmann K-P (2006) Motion perception in rats (*Rattus norvegicus sp.*): deficits in albino Wistar rats compared to pigmented Long-Evans rats. Behav Brain Res 170:29–33

Hupfeld D, Distler C, Hoffmann K-P (2007) Deficits of visual motion perception and optokinetic nystagmus after posterior suprasylvian lesions in the ferret (*Mustela putorius furo*). Exp Brain Res 182(4):509–523

Jeffery G (1997) The albino retina: an abnormality that provides insight into normal retinal development. Trends Neurosci 20:165–169

Kaila K (1994) Ionic basis of $GABA_A$ receptor channel function in the nervous system. Prog Neurobiol 42:489–537

Kakazu Y, Akaike N, Komiyama S, Nabekura J (1999) Regulation of intracellular chloride by cotransporters in developing lateral superior olive neurons. J Neurosci 19:2843–2851

Kittila CA, Massey SC (1997) Pharmacology of directionally selective ganglion cells in the rabbit retina. J Neurophysiol 77:675–689

Langer TP, Lund RD (1974) The upper layers of the superior colliculus of the rat: a Golgi study. J Comp Neurol 158:418–435

Lannou J, Cazin L, Precht W, Toupet M (1982) Optokinetic, vestibular and optokinetic vestibular responses in albino and pigmented rats. Pflügers Arch 393:42–44

Magnin M, Kennedy H, Hoffmann K-P (1989) A double-labeling investigation of the pretectal visuo-vestibular pathways. Vis Neurosci 3:53–58

Morgan JE, Henderson Z, Thompson ID (1987) Retinal decussation patterns in pigmented and albino ferrets. Neurosci 20:519–535

Oyster CW, Simpson JI, Takahashi ES, Soodak RE (1980) Retinal ganglion cells projecting to the rabbit accessory optic system. J Comp Neurol 190:49–61

Palma E, Amici M, Sobrero F, Spinelli G, Di Angelantonio S, Ragozzino D, Mascia A, Scoppetta C, Esposito V, Miledi R, Eusebi F (2006) Anomalous levels of Cl^- transporters in the hippocampal subiculum from temporal lobe epilepsy patients make GABA excitatory. Proc Natl Acad Sci USA 103(22):8465–8468

Paxinos G, Watson C, Pennisi M, Topple A (1985) Bregma, lambda and the interaural midpoint in stereotaxic surgery with rats of different sex, strain and weight. J Neurosci Meth 13:139–143

Priebe NJ, Ferster D (2005) Direction selectivity of excitation and inhibition in simple cells of the cat primary visual cortex. Neuron 45(1):133–145

Rachel RA, Dölen G, Hayes NL, Lu A, Erskine L, Nowakowski RS, Mason CA (2002) Spatiotemporal features of early neurogenesis differ in wildtype and albino mouse retina. J Neurosci 22:4249–4263

Schmidt M, Lewald J, van der Togt C, Hoffmann K-P (1994) The contribution of GABA-mediated inhibition to response properties of neurons in the nucleus of the optic tract in the rat. Eur J NeuroSci 6:1656–1661

Schuerger RJ, Rosenberg AF, Ariel M (1990) Retinal direction-sensitive input to the accessory optic system: an in vitro approach with behavioral relevance. Brain Res 522(1):161–164

Simpson JI (1984) The accessory optic system. Ann Rev Neurosci 7:13–41

Simpson JI, Soodak RE, Hess R (1979) The accessory optic system and its relation to the vestibulocerebellum. Prog Brain Res 50:715–724

Smith RD, Grzywacz NM, Borg-Graham LJ (1996) Is the input to a GABAergic synapse the sole asymmetry in turtle's retinal directional selectivity? Vis Neurosci 13(3):423–439

Sun W, Deng Q, Levick W, He S (2006) On direction-selective ganglion cells in the mouse retina. J Physiol 576:197–202

Taylor WR, He S, Levick WR, Vaney DI (2000) Dendritic computation of direction selectivity by retinal ganglion cells. Science 289:2347–2350

Telkes I, Garipis N, Hoffmann K-P (2001) Morphological changes in the neuronal substrate for the optokinetic reflex in albino ferrets. Exp Brain Res 140:345–356

Thiele A, Distler C, Korbmacher H, Hoffmann K-P (2004) Contribution of inhibitory mechanisms to direction selectivity and response normalisation in macaque area MT. Proc Natl Acad Sci USA 101:9810–9815

Yamada J, Okabe A, Toyoda H, Kilb W, Luhmann HJ, Fukuda A (2004) Cl^- uptake promoting depolarizing GABA actions in immature rat neocortical neurones is mediated by NKCC1. J Physiol 557.3:829–841

Zhang HY, Hoffmann K-P (1993) Retinal projections to the pretectum, accessory optic system and superior colliculus in pigmented and albino ferrets. Eur J NeuroSci 5:486–500